JBC RESEARCH ARTICLE

Transcription regulation by CarD in mycobacteria is guided by basal promoter kinetics

Received for publication, January 23, 2023, and in revised form, March 30, 2023 Published, Papers in Press, April 17, 2023,
https://doi.org/10.1016/j.jbc.2023.104724

Dennis X. Zhu and Christina L. Stallings*

From the Department of Molecular Microbiology, Center for Women's Infectious Disease Research, Washington University School of Medicine, St Louis, Missouri, USA

Reviewed by members of the JBC Editorial Board. Edited by Ursula Jakob

Bacterial pathogens like *Mycobacterium tuberculosis* (*Mtb*) employ transcription factors to adapt their physiology to the diverse environments within their host. CarD is a conserved bacterial transcription factor that is essential for viability in *Mtb*. Unlike classical transcription factors that recognize promoters by binding to specific DNA sequence motifs, CarD binds directly to the RNA polymerase to stabilize the open complex intermediate (RP_o) during transcription initiation. We previously showed using RNA-sequencing that CarD is capable of both activating and repressing transcription *in vivo*. However, it is unknown how CarD achieves promoter-specific regulatory outcomes in *Mtb* despite binding indiscriminate of DNA sequence. We propose a model where CarD's regulatory outcome depends on the promoter's basal RP_o stability and test this model using *in vitro* transcription from a panel of promoters with varying levels of RP_o stability. We show that CarD directly activates full-length transcript production from the *Mtb* ribosomal RNA promoter *rrn*AP3 (AP3) and that the degree of transcription activation by CarD is negatively correlated with RP_o stability. Using targeted mutations in the extended −10 and discriminator region of AP3, we show that CarD directly represses transcription from promoters that form relatively stable RP_o. DNA supercoiling also influenced RP_o stability and affected the direction of CarD regulation, indicating that the outcome of CarD activity can be regulated by factors beyond promoter sequence. Our results provide experimental evidence for how RNA polymerase–binding transcription factors like CarD can exert specific regulatory outcomes based on the kinetic properties of a promoter.

Throughout their life cycle, bacteria must continuously adapt their physiology to respond to and survive in their changing environments. As such, the ability to sense environmental signals and transduce these cues into an appropriate physiological response is important for the virulence of pathogens such as *Mycobacterium tuberculosis* (*Mtb*), which face threats from both the host immune system and antibiotic treatment. Regulation of transcription initiation is a major mechanism by which bacteria adapt their gene expression in response to environmental stimuli. Transcription in bacteria is performed by a single RNA polymerase (RNAP) enzyme, which consists of a multisubunit core enzyme that can bind to different sigma factors (σ) to form a holoenzyme and initiate promoter-specific transcription. *Mtb* devotes a significant fraction of its genome toward encoding numerous transcription factors that can regulate transcription initiation by altering the promoter specificity and recruitment of RNAP (1, 2). Classically, transcription factors are recruited to promoters by recognizing and binding a DNA sequence motif, which allows the factor to specifically regulate a subset of the genome. However, bacteria also encode transcription factors that instead localize to promoter regions by binding directly to RNAP (3, 4). This class of transcription factors is best exemplified by the stringent response regulators DksA and guanosine (penta)tetraphosphate [(p)ppGpp], which bind to the *Escherichia coli* RNAP to directly activate or repress transcription from subsets of *E. coli* promoters (5). These factors exert promoter-specific transcription regulation despite being unable to discriminate promoters at the level of binding. The prevailing hypothesis for the mechanism behind this promoter specificity postulates that these factors can potentiate different outcomes on transcription depending on the underlying initiation kinetics of a promoter (6). Recently, this hypothesis has also been applied to the regulatory mechanisms of other RNAP-binding transcription factors such as CarD (7, 8).

CarD is an RNAP-binding transcription regulator that is widely conserved across many eubacteria phyla and essential for viability in mycobacteria (9). CarD associates with transcription initiation complexes by binding directly to the RNAP β subunit through its N-terminal RNAP-interaction domain (RID) (9, 10). The CarD C-terminal DNA-binding domain (DBD) also interacts with DNA at the upstream fork of the transcription bubble in a sequence-independent manner (11–13). Numerous kinetic studies have demonstrated that CarD stabilizes the RNAP-promoter open complex (RP_o) formed by the mycobacterial RNAP during transcription initiation (13–17). CarD accomplishes this through a two-tiered kinetic mechanism in which it binds to RNAP-promoter closed complexes (RP_c) to increase the rate of DNA melting while also slowing the rate of bubble collapse (15). Furthermore, by stabilizing RP_o, CarD slows the rate of promoter escape (18), which is a necessary step preceding

* For correspondence: Christina L. Stallings, stallings@wustl.edu.

full-length RNA synthesis. Due to its ability to stabilize RP_o *in vitro*, it was expected that CarD functioned generally as a transcription activator. However, although numerous studies have examined CarD's effect on individual rate constants between transcription initiation intermediates (14, 15, 18), the composite effect of CarD's kinetic mechanism on full-length RNA production remains unknown. Furthermore, while *in vitro* studies of CarD have utilized only a handful of promoters, primarily focusing on the *Mtb* ribosomal RNA promoter *rrnA*P3 (AP3) (12–16, 18–20), chromatin immunoprecipitation sequencing (ChIP-seq) in *Mycobacterium smegmatis* indicates that CarD colocalizes with the housekeeping sigma factor σ^A to promoter regions broadly across the mycobacterial genome (17, 21), leaving a gap in our understanding of CarD's activity under different promoter contexts.

To characterize CarD's role in transcription regulation throughout the mycobacterial genome, we previously performed RNA-sequencing (RNA-seq) on a set of *Mtb* strains expressing mutants of CarD that either impair or enhance its ability to stabilize RP_o *in vitro* (8). We discovered that altering CarD activity in *Mtb* led to both upregulation and downregulation of numerous protein-encoding transcripts, suggesting that CarD could function as either a transcriptional activator or a transcriptional repressor in different promoter contexts. Prior *in vitro* studies with *Rhodobacter sphaeroides* CarD and RNAP have shown that *Rsp*CarD activates transcription from promoters lacking a conserved T at the −7 position (22) and represses transcription from its own promoter (23). However, unlike Alphaproteobacteria like *R. sphaeroides*, which contain a T_{-7} at fewer than 50% of their promoters, most other bacterial phyla, including Actinobacteria like *Mtb*, have a T_{-7} at over 90% of their promoters (22), making it unlikely that the T_{-7} is a conserved mechanism of CarD promoter specificity. Instead, we previously proposed a model in which the outcome of CarD regulation is dependent on the basal transcription initiation kinetics at a given promoter (7, 8). Specifically, at unstable promoters that are rate limited at the step of bubble opening, CarD would facilitate full-length RNA production by stabilizing RP_o, while at stable promoters that are rate limited at the step of promoter escape, CarD would make it more difficult for RNAP core enzyme to break contacts with promoter DNA. Herein, we directly test our model using *in vitro* transcription approaches to explore the relationship between RP_o stability and transcription regulation by CarD. We discover that both promoter DNA sequence and DNA topology influence the basal RP_o stability of a promoter and the regulatory outcome of CarD on transcription. In addition, we find that in the context of a promoter with high basal RP_o stability, CarD can directly repress transcription, marking the first demonstration of direct transcriptional repression by *Mtb* CarD. This work provides experimental evidence for how RNAP-binding transcription factors like CarD can potentiate multiple regulatory outcomes on transcription through a single kinetic mechanism.

Results

CarD binding correlates with transcriptional regulation but not the direction of regulatory outcome

A fundamental feature in our model of CarD mechanism is that the regulatory outcome of CarD on a given mycobacterial promoter is determined based on differences in the basal transcription initiation kinetics of the promoter and not differences in CarD binding. This model is based on comparing ChIP-seq data from *M. smegmatis*, where CarD is present at almost all RNAP-σ^A transcription initiation complexes (17, 21), with RNA-seq data from *Mtb*, where mutation of CarD resulted in both upregulation and downregulation of gene expression (8). However, we cannot yet rule out the alternative hypothesis that CarD's uniform localization pattern in *M. smegmatis* represents a unidirectional transcription activating mechanism for CarD in *M. smegmatis* in contrast to the bi-directional regulatory activity in *Mtb* that is suggested by our RNA-seq data.

To address this gap in our model, we performed an RNA-seq experiment in *M. smegmatis* that could be directly compared to the *M. smegmatis* ChIP-seq dataset. In our published *Mtb* RNA-seq experiment (8), we collected RNA from *Mtb* strains expressing mutant alleles of CarD with either weakened affinity for RNAP ($CarD^{R47E}$), predicted weakened affinity for DNA ($CarD^{K125A}$), or increased affinity for RNAP ($CarD^{I27F}$ and $CarD^{I27W}$). By collecting RNA from *Mtb* strains with mutations that target different domains of CarD, we were able to dissect how the respective interactions of CarD's functional domains contributed to its role in regulating the *Mtb* transcriptome. To replicate this experimental design in *M. smegmatis*, we collected RNA from four strains of *M. smegmatis* with the native copy of *carD* deleted and expressing one of four different alleles of *Mtb* CarD: wildtype (WT) CarD ($CarD^{WT}$), $CarD^{R25E}$ (a RID mutant with weakened affinity for RNAP), $CarD^{K125E}$ (a DBD mutant with weakened affinity for DNA), or $CarD^{I27W}$ (a RID mutant with increased affinity to RNAP) as the only *carD* allele (Table S1). Similar to the CarD mutations used in our *Mtb* experiment, the CarD mutations that weaken its macromolecular interactions with RNAP or DNA (R25E and K125E) impair CarD's ability to stabilize RP_o *in vitro* (13, 15), while the I27W mutation increases its affinity for RNAP and allows CarD to potentiate RP_o stabilization at lower concentrations (20). For each strain, we collected RNA from four biological replicates of exponentially growing cells in nutrient replete conditions for sequencing. Two replicates ($CarD^{R25E}$-1 and $CarD^{K125E}$-4) were identified as outliers following principal component analysis (PCA) and were discarded from downstream analysis (Fig. S1).

In all three strains with mutations in *carD*, over 25% of the 6716 coding genes in *M. smegmatis* Mc^2155 were significantly differentially expressed ($P_{adj} < 0.05$) in comparison to the $CarD^{WT}$ strain (Fig. 1*A* and Table S1). The number of differentially expressed genes in the $CarD^{R25E}$ (2909 genes) and $CarD^{K125E}$ (2901 genes) *M. smegmatis* strains is similar to the

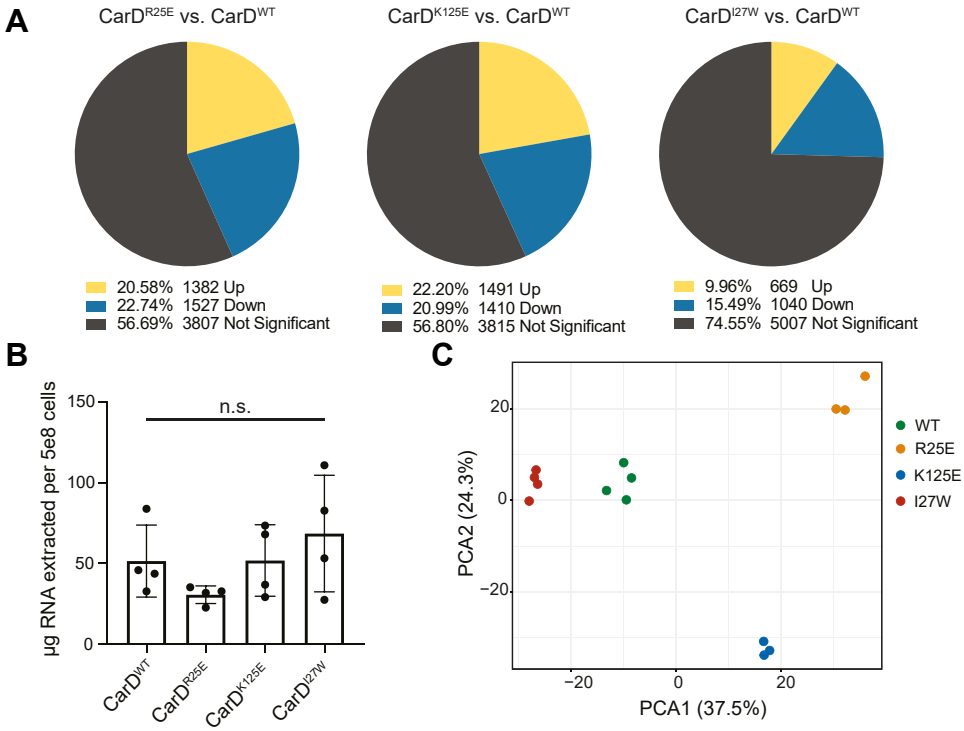

Figure 1. *M. smegmatis* strains encoding point mutants of CarD display broad changes in transcript expression. *A*, pie charts displaying the percentage of *M. smegmatis* coding genes that were significantly differentially expressed ($p_{adj} < 0.05$) in each CarD mutant strain relative to CarD^{WT}. *B*, RNA content for *M. smegmatis* strains expressing different alleles of CarD calculated from total RNA weight harvested from four biological replicates divided by estimated number of cells collected. Each bar represents the mean ± standard deviation (SD). Group means were compared using a one-way ANOVA and determined to be not significantly different ($p = 0.228$). *C*, principal component analysis of RNA sequencing samples based on read counts of 6716 *M. smegmatis* MC^{2}155 coding genes. The first two principal components (PC1 and PC2), which account for 37.5% and 24.3% of the variance, respectively, define the x- and y-axis, respectively.

number of differentially expressed genes in the CarD^{R47E} (2877 genes) and CarD^{K125A} (2690 genes) *Mtb* strains (8). However, homologous genes between the two species showed little correlation in their transcript expression patterns (Fig. S2 and Table S2), suggesting that CarD does not simply regulate a subset of homologous genes conserved between *Mtb* and *M. smegmatis*. Each of the *M. smegmatis* CarD mutant strains exhibited a similar number of upregulated genes as downregulated genes (Fig. 1*A*), following the same pattern as the *Mtb* CarD mutant strains (8) and suggesting that CarD is capable of potentiating both transcriptional activation and repression in *M. smegmatis*. Importantly, the strains did not show significant differences in the total amount of RNA per cell (Fig. 1*B*), suggesting that the transcript abundance differences measured in the CarD mutant strains represent local changes in transcription at specific genes rather than a global decrease in RNA production within the cell that would be expected if CarD functioned strictly as a transcriptional activator.

The transcriptomic relationship between different CarD mutant strains in *M. smegmatis* was also consistent with the relationships we observed in our *Mtb* dataset (8). PCA of the RNAseq data illustrated that the *M. smegmatis* sample replicates clustered tightly with each other based on CarD genotype and samples from CarD mutant strains with impaired RP_o-stabilizing activity (CarD^{R25E} and CarD^{K125E}) separated from the strain with enhanced RP_o-stabilizing activity (CarD^{I27W}) along the first principal component (Fig. 1*C*), demonstrating consistency between replicates from the same genotype and suggesting that altered CarD RP_o-stabilizing activity contributes to transcript abundance changes in the mutant bacteria. In addition, the CarD^{R25E} and CarD^{I27W} strains, which encode CarD RID mutants with impaired or enhanced RP_o-stabilization *in vitro*, respectively, displayed largely opposite transcriptomic changes (Fig. S3*A*), similar to the RID mutants in *Mtb* (8). In the PCA, the CarD^{K125E} samples separated from all other samples along the second principal component (Fig. 1*A*) and the direction of transcript abundance changes in the DBD mutant CarD^{K125E} samples correlated poorly with the transcript abundance changes in the RID mutant CarD^{R25E} samples ($R^2 = 0.351$) (Fig. S3, *B* and *C*). This is in contrast to the tight correlation between CarD RID and DBD mutants in *Mtb* (8) and may suggest that mutations in the DBD and RID have unique effects on CarD's regulatory function in *M. smegmatis*.

The ChIP-seq dataset shows that CarD is present when RNAP-σ^A is also found, supporting a model that CarD is present at the promoters of both upregulated and downregulated genes. However, our data are also compatible with an alternative model in which CarD acts directly as a monotonic transcriptional activator, and genes that appear to be transcriptionally "repressed" by CarD are expressed at lower levels in WT bacteria due to decreased RNAP occupancy at non-CarD-activated promoters. If this alternative model were true, then we would expect to find RNAP-σ^A/CarD binding

sites overlapping with transcription start sites (TSSs) ascribed to the transcriptionally "activated" promoters but absent from TSSs ascribed to transcriptionally "repressed" promoters. To examine the overlap between CarD binding sites and CarD-regulated transcripts, we used our RNA-seq dataset to identify a list of *M. smegmatis* genes whose transcript abundance was likely directly responsive to altered CarD-mediated RP_o stabilization activity based on having opposite expression patterns in $CarD^{R25E}$ *versus* $CarD^{I27W}$. To avoid internal genes within operons, we focused our analysis on 2917 *M. smegmatis* genes directly downstream of a primary TSS (24) and categorized them into one of four classes (Table S3). TSSs associated with genes that were significantly downregulated ($P_{adj} < 0.05$) in $CarD^{R25E}$ and significantly upregulated in $CarD^{I27W}$ were classified as 'Activated' by CarD (n = 117), while TSSs associated with genes that were significantly upregulated in $CarD^{R25E}$ and significantly downregulated in $CarD^{I27W}$ were classified as 'Repressed' by CarD (n = 153). TSSs associated with genes that were significantly differentially expressed in both $CarD^{R25E}$ and $CarD^{I27W}$ but in the same direction relative to wildtype were classified as 'Uncategorized' (n = 222) because their expression profile does not reflect the divergent expression pattern expected between CarD mutants with opposing effects on RP_o-stabilization *in vitro*. Lastly, any TSSs that were not significantly differentially expressed in both $CarD^{R25E}$ and $CarD^{I27W}$ were categorized as 'Not Significant' (n = 2425).

We reanalyzed our previous ChIP-seq dataset (17, 21) and identified 1857 unique CarD binding sites across two biological replicates (Table S3). To avoid broad binding regions that may represent multiple, overlapping CarD binding sites, we focused on 1796 CarD binding sites less than or equal to 1000 base pairs (bp) in width. Of these 1796 CarD binding sites, 1390 sites (77.4%) overlapped with at least one mapped TSS in *M. smegmatis* and 1129 sites (62.8%) overlapped with a primary TSS associated with a protein-encoding gene (24). We examined the overlap between CarD binding sites and TSSs that were significantly differentially expressed in both $CarD^{R25E}$ and $CarD^{I27W}$ and found that 57.9% (285/492) of these TSSs were associated with CarD binding (Table 1). Among the differentially expressed genes, 53.0% (62/117) of 'Activated' TSSs and 67.3% (103/153) of 'Repressed' TSSs overlapped with a CarD binding site (Table 1). Thus, CarD binding is associated with transcriptional regulation of *M. smegmatis* promoters *in vivo* but is not correlated with the direction of regulation. A similar analysis was performed in the α-proteobacterium *Caulobacter crescentus* to identify the direct regulon of CdnL (the *C. crescentus* homolog of CarD) (25). Like our results, CdnL localized to promoter regions of both genes that were upregulated and genes that were downregulated in a Δ*cdnL* strain, but a vast majority of differentially expressed genes were not associated with CdnL binding, suggesting a broader effect of indirect regulation in *C. crescentus*. Together, these data support the model that CarD is broadly localized to mycobacterial promoters through its interaction with RNAP but that the regulatory outcome of CarD activity is not determined by occupancy.

CarD directly activates transcription from the Mtb *ribosomal RNA promoter* rrn*AP3*

To test our model that the outcome of CarD's RP_o stabilizing activity on transcript production depends on the basal promoter kinetics, we used *in vitro* transcription methods to measure the direct effects of CarD on transcript production. Although several studies have proposed that CarD activates transcription from the *Mtb* AP3 promoter based on *in vitro* three-nucleotide transcription assays (16, 20) and real-time fluorescence assays (14, 15) that report RP_o lifetime, full-length transcript production has never been directly measured. To assess full-length RNA production, we performed multiround *in vitro* transcription assays by incubating recombinantly purified *Mtb*RNAP-σ^A holoenzyme with a linear DNA fragment containing the *Mtb* AP3 promoter (from −39 to +4 with respect to the TSS) driving transcription of a 164 nucleotide RNA product. The addition of a saturating concentration of WT CarD (25:1 M ratio CarD:RNAP (15)) activated transcription from the AP3 promoter ∼8-fold compared to reactions with no factor added (Fig. 2*A*). To investigate how CarD's RP_o-stabilizing activity relates to transcriptional activation, we repeated the multiround *in vitro* transcription assays with CarD mutants impaired in their ability to stabilize RP_o *in vitro* ($CarD^{R25E}$, $CarD^{R47E}$, $CarD^{K125A}$, and $CarD^{K125E}$) (13, 15). All four of the CarD mutants activated transcription from AP3 compared to reactions with no factor, but the degree of activation by each mutant was reduced compared to WT CarD (Fig. 2*A*), suggesting that CarD's RP_o-stabilizing activity underlies its ability to activate transcription from AP3. In addition, the degree to which each CarD mutant attenuated transcript production correlated with how severe the impact was on the CarD macromolecular interactions with RNAP (10) or DNA (13). In contrast, $CarD^{I27W}$, which has increased affinity for RNAP and is able to stabilize RP_o at lower concentrations than $CarD^{WT}$ (20), activated transcription from AP3 to a greater degree than $CarD^{WT}$ at concentrations below

Table 1
CarD binding is associated with both activated and repressed transcription start sites (TSSs)

TSS category	Differentially Expressed			Not Significant	TOTAL
	Activated	Repressed	Uncategorized		
Overlapping with CarD binding site	62 (53.0%)	103 (67.3%)	120 (54.0%)	1089 (44.9%)	1374 (47.1%)
Total # TSSs	117	153	222	2425	2917

'Differentially Expressed' TSSs are those TSSs associated with genes that were significantly differentially expressed ($p_{adj}<0.05$) in both $CarD^{R25E}$ and $CarD^{I27W}$ relative to $CarD^{WT}$. A differentially expressed gene was categorized as: 'Activated' if it was down-regulated in $CarD^{R25E}$ and up-regulated in $CarD^{I27W}$, 'Repressed' if it was up-regulated in $CarD^{R25E}$ and down-regulated in $CarD^{I27W}$, or 'Uncategorized' if it was differentially expressed in the same direction in both mutant strains. TSSs associated with genes that were not significantly differentially expressed in both mutant strains were categorized as 'Not Significant'. The percent of total TSSs in a given category that overlapped with a CarD binding site is shown in the parentheses.

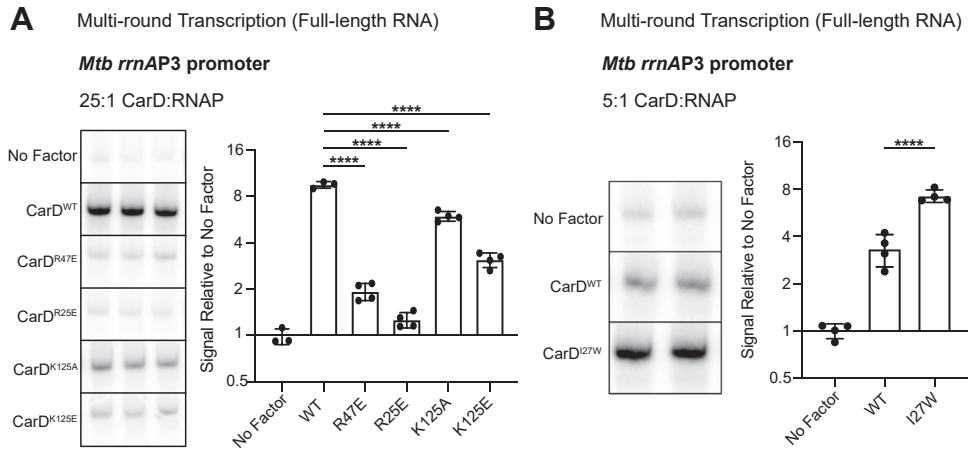

Figure 2. CarD activates transcription from the *Mtb* ribosomal RNA promoter AP3, and mutations to either the RNA polymerase (RNAP) interaction domain (RID) or DNA-binding domain (DBD) affect this activity *in vitro*. *A*, representative gel images from multiround *in vitro* transcription reactions of *Mtb*RNAP-σ^A holoenzyme on linear DNA templates encoding AP3 with either no factor, wildtype CarD ($CarD^{WT}$), one of two RID mutants ($CarD^{R47E}$ or $CarD^{R25E}$), or one of two DBD mutants ($CarD^{K125A}$ or $CarD^{K125E}$). In all reactions with factor, CarD is added at a 25:1 M ratio to RNAP holoenzyme. The bar graph displays the mean transcript signal intensity relative to 'No Factor' ± standard deviation (SD). N = 3 to 4 independent reactions for each condition. *B*, representative gel images from multiround *in vitro* transcription reactions of *Mtb*RNAP-σ^A holoenzyme on AP3 with either no factor, $CarD^{WT}$, or a RID mutant with higher affinity for RNAP ($CarD^{I27W}$). In all reactions with factor, CarD is added at a subsaturating concentration of 5:1 M ratio to RNAP holoenzyme. The bar graph displays the mean transcript signal intensity relative to 'No Factor' ± SD. N = 4 independent reactions for each condition. *A* and *B*, Mean fold-change values were compared using a one-way ANOVA followed by post-hoc Dunnett's tests comparing the mean of each mutant CarD allele to $CarD^{WT}$; **** = $p < 0.0001$. The full ANOVA results are listed in Table S4. The raw gel images directly from the phosphorimager are shown in Fig. S6. AP3, *Mtb* ribosomal RNA promoter *rrn*AP3; *Mtb, Mycobacterium tuberculosis*.

where $CarD^{WT}$ is saturating (5:1 M ratio CarD:RNAP) (Fig. 2*B*), further demonstrating the association between CarD's RP_o-stabilizing activity and activation of transcript production. Collectively, these results demonstrate that CarD activates full-length RNA production *in vitro* from AP3 and this transcription activation is dependent on the RP_o-stabilizing activity of CarD.

Additional promoter DNA–RNAP interactions increase basal RP_o stability and push CarD toward transcriptional repression

To test the hypothesis that the degree of transcriptional activation by CarD is inversely correlated with the basal RP_o stability of a promoter, we explored CarD's direct regulatory effect on transcription from a set of promoters with varying levels of basal RP_o stability. Transcription initiation kinetics and RP_o lifetime are highly dependent on promoter DNA sequence (26). In the RP_o intermediate, the promoter DNA makes multiple sequence-specific contacts with regions of the RNAP holoenzyme to stabilize the transcription bubble (26–28). The *Mtb* RNAP-σ^A holoenzyme and WT AP3 ($AP3_{WT}$) promoter form a relatively unstable RP_o (15, 16) that is stabilized by CarD to lead to activation of transcription *in vitro* (Fig. 2). We, therefore, used the AP3 promoter sequence as a starting point to generate four additional promoter templates ($AP3_{EcoExt}$, $AP3_{MycoExt}$, $AP3_{Discr}$, and $AP3_{Stable}$) with higher levels of basal RP_o stability by making targeted sequence mutations that would add or optimize predicted DNA–RNAP interactions in RP_o (Fig. 3*A*). $AP3_{WT}$ contains near consensus sequence motifs in the −35 and −10 elements (29), which are highly conserved promoter elements that interact with σ region 4 and 2, respectively (30–32), so we did not target these regions in our study. In $AP3_{EcoExt}$, we mutated the base at position −14 to a G to introduce a $T_{-15}G_{-14}$ motif that represents an extended −10 element that was first identified in *E. coli* (33). In addition to the classical *E. coli*-like extended −10 motif, many mycobacterial promoters instead contain a G at position −13 that is associated with promoter strength and RP_o formation in DNase I footprinting studies (34). Thus, we also generated $AP3_{MycoExt}$, which is mutated to include a G_{-13} upstream of the −10 element. Both G_{-14} and G_{-13} are positioned to interact with a conserved glutamic acid residue in σ^A region 3.0 in the mycobacterial RP_o (14, 34, 35). $AP3_{Discr}$ is mutated to introduce a $G_{-6}GGA_{-3}$ motif in the discriminator region immediately downstream of the −10 hexamer that allows for optimal binding with σ^A region 1.2 (36–38). $AP3_{Stable}$ is mutated to include the mutations made in $AP3_{EcoExt}$ and $AP3_{Discr}$ as well as a deletion of a T at position −17 to reduce the length of the spacer region between the −35 and −10 hexamers from 18-bp in $AP3_{WT}$ to 17-bp. A spacer length of 17 bp allows for optimal interactions of the −35 and −10 hexamers with σ^A (39).

To measure the basal RP_o stability of RNAP-σ^A and the AP3 promoter variants, we performed *in vitro* three-nucleotide transcription initiation assays (16, 20) in the absence of CarD by incubating *Mtb*RNAP-σ^A holoenzyme with linear promoter DNA fragments in the presence of a GpU dinucleotide and UTP. In these reactions, the RNAP-σ^A holoenzyme can synthesize a three nucleotide 'GUU' RNA transcript but cannot undergo promoter escape, allowing us to assess relative RP_o lifetimes by using the amount of three nucleotide product as a proxy. We found that all the promoter variants with additional predicted DNA–RNAP contacts exhibited higher basal levels of RP_o stability compared to $AP3_{WT}$ (Fig. 3*B*). The most stable variant $AP3_{Stable}$ displayed 8-fold higher basal RP_o stability relative to $AP3_{WT}$. To quantify the effect of CarD on RP_o stability from these promoter variants, we also performed three-nucleotide transcription assays in the presence of WT

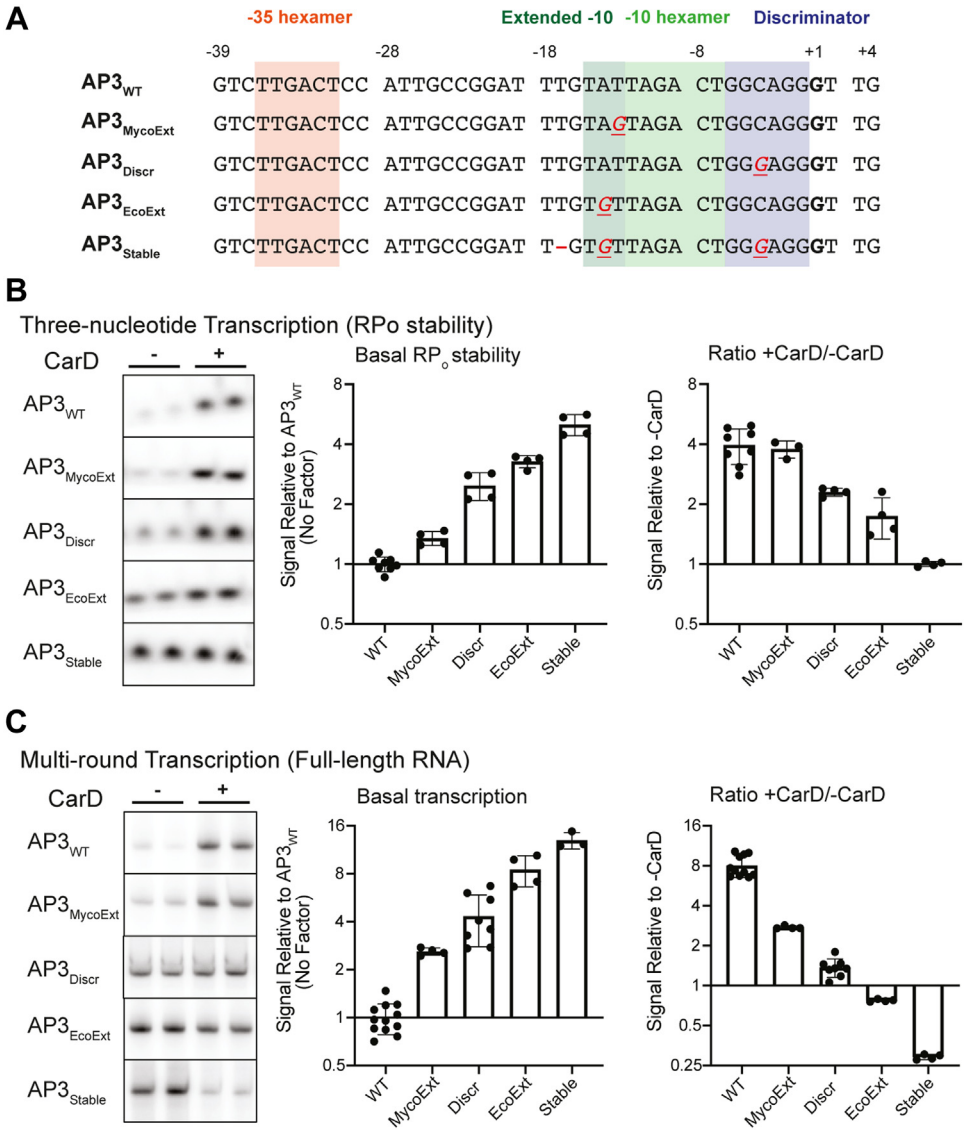

Figure 3. Promoter sequences that introduce additional interactions between promoter DNA and RNAP in the open complex increase basal RP_o stability and shift the regulatory outcome of CarD toward transcriptional repression. *A*, promoter sequences of the wildtype *Mtb rrn*AP3 promoter ($AP3_{WT}$) and four variants with sequence mutations that add predicted interactions between promoter DNA and RNAP in RP_o. Sequences from the −39 to +4 position relative to the transcription start site (+1, *bolded*) are shown. In the non-WT sequences, DNA bases that are altered from the WT sequence are underlined and colored *red*. A "—" indicates that a base was deleted. *B*, representative gels showing [^{32}P]-labeled three-nucleotide transcription products formed by *Mtb*RNAP-σ^A from linear DNA templates encoding $AP3_{WT}$ or one of the four AP3 variants either in the absence or presence of CarD. *C*, representative gels from multiround transcription assays showing 164 nucleotide [^{32}P]-labeled RNA transcripts produced by *Mtb*RNAP-σ^A from linear DNA templates encoding $AP3_{WT}$ or one of the four AP3 variants either in the absence or presence of CarD. *B* and *C*, bar graphs display (*left*) the mean basal signal intensity relative to $AP3_{WT}$ ± standard deviation (SD) and (*right*) the mean ratio of signal intensity +CarD/-CarD for each promoter ± SD. Group means were compared by one-way ANOVA $p < 0.0001$. The full results of pairwise comparisons are listed in Table S4. The raw gel images directly from the phosphorimager are shown in Figs. S5 and S6. AP3, *Mtb* ribosomal RNA promoter *rrn*AP3; *Mtb, Mycobacterium tuberculosis*; RNAP, RNA polymerase; RP_o, RNAP-promoter open complex.

CarD protein (Fig. 3*B*). On $AP3_{WT}$, CarD increased the amount of three nucleotide product by roughly 4-fold over reactions with no factor. As the basal RP_o stability of promoter variants increased, the degree of RP_o stabilization by CarD decreased to the point that on $AP3_{Stable}$, the addition of CarD resulted in no detectable difference in the amount of three nucleotide product.

Having established a set of promoters with different basal RP_o stability levels that range over nearly one order of magnitude, we performed multiround *in vitro* transcription reactions using these AP3 promoter variants in the presence or absence of CarD to investigate the relationship between the basal RP_o stability of a promoter and transcriptional regulation by CarD (Fig. 3*C*). We discovered that across the AP3 promoter variants, basal RP_o stability positively correlated with full-length transcript production in the absence of CarD but negatively correlated with transcriptional activation by CarD. Indeed, the two promoters with the highest levels of basal RP_o stability ($AP3_{EcoExt}$ and $AP3_{Stable}$) were transcriptionally repressed by CarD, consistent with the predictions of our model and providing the first *in vitro* evidence of direct transcription repression by *Mtb* CarD.

Basal RP_o stability and CarD regulatory outcome are influenced by discriminator region guanosine + cytosine base pair frequency

In addition to forming direct interactions with the polymerase, promoter DNA sequences can also influence RP_o stability by affecting the chemical properties of the DNA molecule. For example, guanosine + cytosine base pairs in the discriminator region impose a kinetic barrier to DNA untwisting and unwinding during the formation of the transcription bubble due to their greater base-pairing and base-stacking stability compared to adenosine + thymine base pairs (40, 41). Discriminator guanosine + cytosine base pair frequency (G + C%) is inversely correlated with RP_o stability (42) and has been shown to be a determinant of transcription control by DksA/(p)ppGpp (5, 43). To determine if changing the RP_o stability by modifying the G + C% of the discriminator affects the outcome of CarD activity on transcript production, we generated a set of AP3 promoter variants ($AP3_{Discr1}$ – $AP3_{Discr5}$) in which the discriminator region G + C% is titrated from 100% ($AP3_{Discr1}$) to 16.7% ($AP3_{Discr5}$) (Fig. 4*A*). We

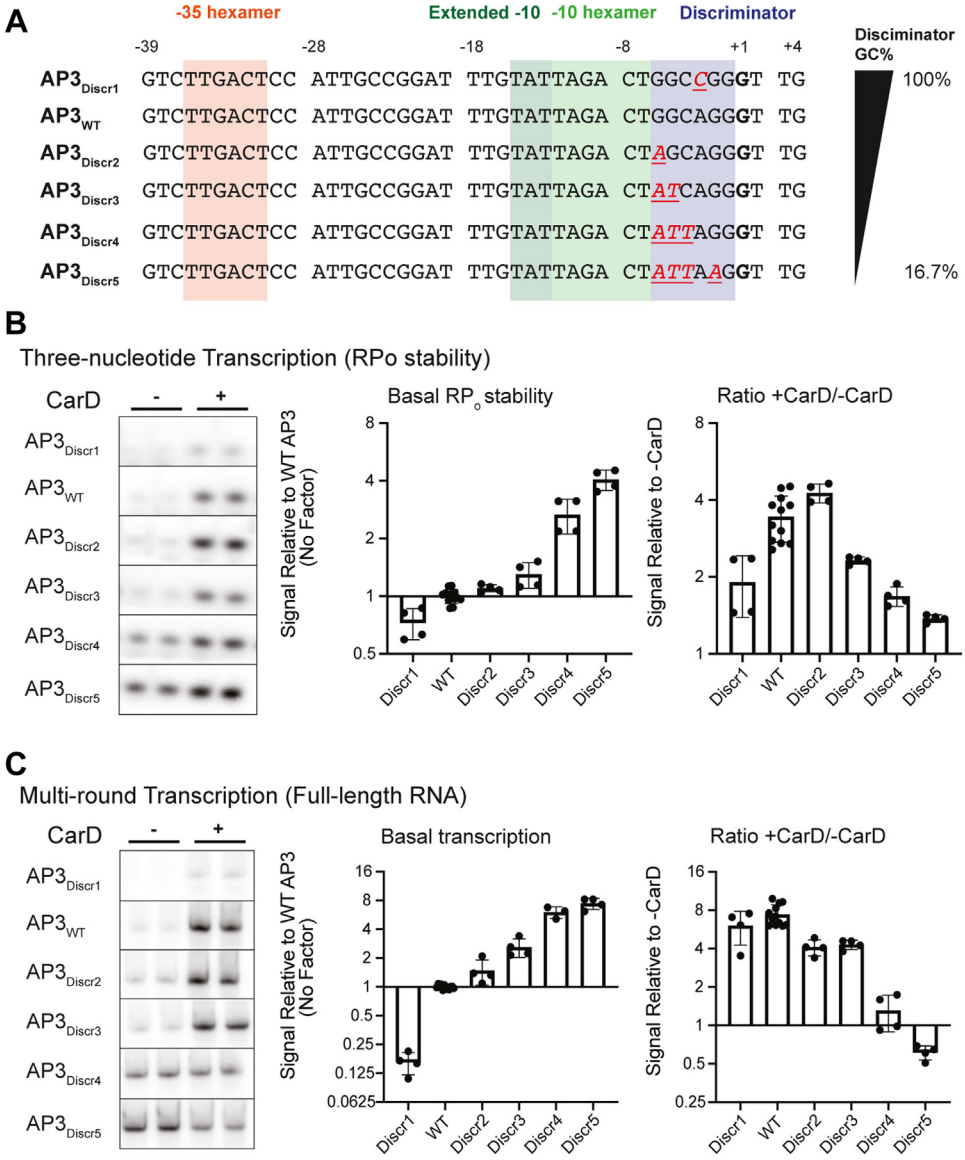

Figure 4. Discriminator GC% negatively correlates with basal RP_o stability and influences CarD regulatory outcome. *A*, promoter sequences of the wildtype *Mtb rrn*AP3 promoter ($AP3_{WT}$) and five variants with sequence mutations that either increase or decrease the percentage of G or C bases in the discriminator. Sequences from the −39 to +4 position relative to the transcription start site (+1, *bolded*) are shown. In the non-WT sequences, DNA bases that are altered from the WT sequence are underlined and colored *red*. *B*, representative gels showing [^{32}P]-labeled three-nucleotide transcription products formed by *Mtb*RNAP-σ^A from linear DNA templates encoding $AP3_{WT}$ or one of the five AP3 variants either in the absence or presence of CarD. *C*, representative gels from multiround transcription assays showing 164 nucleotide [^{32}P]-labeled RNA transcripts produced by *Mtb*RNAP-σ^A from linear DNA templates encoding $AP3_{WT}$ or one of the five AP3 variants either in the absence or presence of CarD. *B* and *C*, bar graphs display (*left*) the mean basal signal intensity (in the absence of CarD) relative to $AP3_{WT}$ ± standard deviation (SD) and (*right*) the mean ratio of signal intensity +CarD/-CarD for each promoter ± SD. Group means were compared by one-way ANOVA $p < 0.0001$. The full results of pairwise comparisons are listed in Table S4. The raw gel images directly from the phosphorimager are shown in Figs. S5 and S6. AP3, *Mtb* ribosomal RNA promoter *rrn*AP3; *Mtb, Mycobacterium tuberculosis*; RP_o, RNAP-promoter open complex.

observed a negative correlation between discriminator G + C% and basal RP_o stability as measured by three-nucleotide transcription assays (Fig. 4*B*). CarD increased three nucleotide RNA production from all promoter variants tested, but the magnitude of RP_o stabilization by CarD displayed a negative correlation with basal RP_o stability across AP3 variants as the discriminator G + C% was titrated (Fig. 4*B*).

Discriminator G + C% of the AP3 variants was also negatively correlated with basal transcript production in the multiround transcription assay and the magnitude of transcription activation by CarD decreased as discriminator G + C% decreased (Fig. 4*C*). On the AP3 variant with the lowest discriminator G + C% and highest basal RP_o stability ($AP3_{Discr5}$), CarD decreased transcript production, further supporting that promoters with high basal RP_o stability can be transcriptionally repressed by CarD. Collectively, our experiments show that promoter sequence motifs that increase basal RP_o stability decrease the magnitude of transcriptional activation by CarD and can lead to transcriptional repression in the most stable RP_o contexts.

Promoter sequences that form more stable RP_o are associated with transcription repression by CarD in vitro *and* in vivo

We show that base substitutions in the spacer region, extended −10 region (Fig. 3), and discriminator (Fig. 4) can affect full-length transcript production and the direction of CarD regulation. To directly examine whether differences in relative RP_o stability could explain the outcomes in transcript production and CarD regulation, we performed a linear regression analysis across all of our promoter templates (Fig. 5). For this analysis, the relative RP_o stability and relative transcription strength of each promoter variant was normalized to $AP3_{WT}$. In the absence of CarD, the rate of full-length transcript production shows a roughly linear positive correlation with the relative RP_o stability (Fig. 5*A*). In contrast, the $\log_2$ ratio of transcript production in multiround transcription reactions ± CarD shows a roughly linear inverse correlation with increasing RP_o stability, with the most stable promoter variants ($AP3_{EcoExt}$, $AP3_{Stable}$, and $AP3_{Discr5}$) being transcriptionally repressed by CarD (Fig. 5*B*). The robust relationship across multiple promoter variants suggests that RP_o stability is a fundamental determinant of full-length transcript production and CarD regulatory outcome. Collectively, our experiments illustrate a relationship between RP_o stability, transcription strength, and CarD regulation and demonstrate that transcription factors like CarD can discriminate promoters based on their basal kinetic features to potentiate bidirectional outcomes in transcription regulation *via* a single kinetic mechanism.

Through our *in vitro* transcription experiments, we have identified multiple promoter sequence motifs associated with high RP_o stability *in vitro*. If our model is generally applicable to transcription from mycobacterial promoters throughout the genome, then we would expect to find an association between DNA sequence motifs associated with RP_o stability and transcriptional repression by CarD. To interrogate this prediction, we examined the prevalence of a consensus extended −10 motif ($T_{-15}G_{-14}N_{-13}$) and discriminator GC% in promoters that were differentially expressed in *our Mtb* and *M. smegmatis* RNA-seq datasets (Table S5). Since all of our *in vitro* experiments were performed in the context of a *Mtb*RNAP-σ^A holoenzyme, we limited our bioinformatic analysis to promoters containing a $A_{-11}NNNT_{-7}$ motif representing the consensus σ^A −10 element (24, 29, 44, 45), which comprised 90.5% (1609/1778) and 82.5% (2511/3043) of the primary TSSs in *Mtb* (44) and *M. smegmatis* (24), respectively. Indeed, in *Mtb*, promoters that were predicted to be repressed by CarD based on our RNA-seq data were overenriched for extended −10 elements, while promoters predicted to be activated by CarD were underenriched for extended −10 elements relative to the genome-wide proportion of this feature (Fig. S4*A*). A similar trend was true of the proportion of promoters containing extended −10 elements in *M. smegmatis*, but the difference in proportions between CarD-regulated promoters and the genome-wide distribution was not

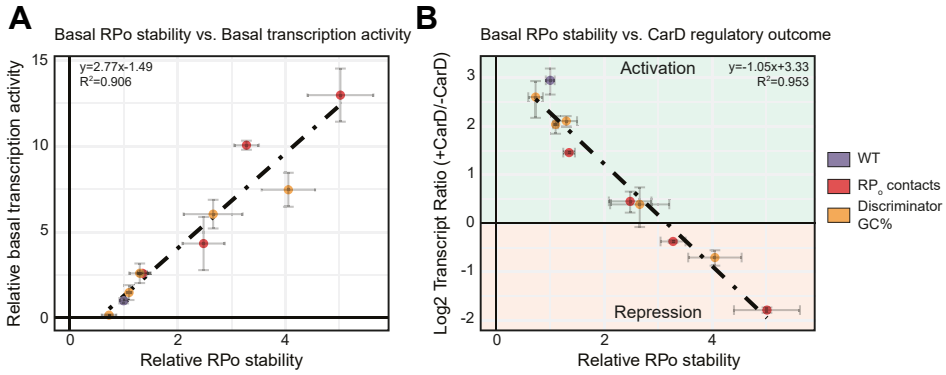

Figure 5. The basal RP_o stability of a promoter is positively correlated with basal transcription activity but negatively correlated with transcription activation by CarD. *A*, *dot plot* showing the relationship between the basal RP_o stability of AP3 promoter variants relative to $AP3_{WT}$ on the x-axis *versus* basal transcription activity relative to $AP3_{WT}$ on the y-axis. Each point represents a variant of the AP3 promoter and is colored based on whether it represents the WT promoter, a sequence with mutations that affect RNAP–DNA interactions in RP_o (RP_o contacts) or a sequence with mutations that affect the discriminator region GC% (Discriminator GC%). The position of each point represents the mean values from at least N = 4 experiments, and the error bars represent standard deviations. The *dashed line* and *text* represent the results of a linear regression analysis. *B*, *dot plot* showing the relationship between the basal RP_o stability of AP3 promoter variants *versus* the $\log_2$ ratio of transcript production in reactions ± CarD on the y-axis. Positive '$\log_2$ Transcript Ratio' values indicate transcription activation while negative values indicate transcriptional repression. AP3, *Mtb* ribosomal RNA promoter *rrnAP3*; RNAP, RNA polymerase; RP_o, RNAP-promoter open complex.

statistically significant (Fig. S4*B*). In both species, promoters that were predicted to be repressed by CarD contained significantly more GC-rich discriminator regions than promoters predicted to be activated by CarD (Fig. S4, *C* and *D*). The association of stable RP_o DNA sequence signatures with genes that are inferred to be repressed by CarD *in vivo* support that the regulatory mechanisms that we demonstrate *in vitro* could be relevant to gene expression *in vivo*.

DNA topology can influence the regulatory outcome of CarD activity

In mycobacteria, CarD transcript levels increase in response to double-stranded DNA breaks and genotoxic stress (9), suggesting that the dynamics of CarD regulation may be important for responding to these environmental cues. DNA breaks in the chromosome can relieve local regions of DNA supercoiling. The supercoiling state of promoters is tightly connected to transcriptional activity *in vivo*, as positive or negative supercoiling can inhibit or enhance RP_o formation, respectively (46,47). Thus, we sought to test the relationship between promoter topology and CarD regulation. We generated a set of templates with identical DNA sequence but varied molecular topology by cloning the $AP3_{WT}$ promoter into a negatively supercoiled plasmid and incubating the plasmid with either a single-cutting endonuclease to produce a linear "cut" DNA molecule, a nicking endonuclease to produce a circular "nicked" DNA molecular, or with no enzyme to maintain a supercoiled control (mock treated) (Fig. 6*A*). We performed *in vitro* three-nucleotide transcription assays using the topologically distinct DNA templates and found that negative supercoiling contributes to a ~6-fold increase in basal RP_o stability compared to a linear "cut" DNA template containing the same promoter sequence (Fig. 6*B*). In addition, the "nicked" DNA template exhibited a similar basal RP_o stability to the "cut" DNA template, indicating that the higher RP_o stability observed in the "mock" template is a result of supercoiling and not the circular shape of the molecule. The addition of CarD decreased the amount of three nucleotide transcript produced with the supercoiled "mock" DNA template. This result could indicate that CarD inhibits progression from RP_o toward an initial transcribing complex intermediate (RP_{itc}) that synthesizes the three nucleotide product quantified in these assays (18). The basal RP_o stabilities of the "cut", "nicked", and "mock" $AP3_{WT}$ DNA templates correlated with the basal transcriptional activity of the promoter, where promoter templates with high basal RP_o stability also showed high levels of basal transcript production (Fig. 6*C*). Furthermore, CarD activated transcription from the "cut" and "nicked" DNA templates but repressed transcription from the supercoiled "mock" DNA template, which has a higher basal RP_o stability relative to the "cut" and "nicked" molecules. These data demonstrate a single promoter DNA sequence can exhibit varying levels of basal RP_o stability based on DNA supercoiling, and this supercoiling-dependent change in RP_o stability can change the regulatory outcome of CarD on transcription. While the DNA sequence of a given promoter is constant within the genome, the topology of the DNA molecule can change over the lifetime of the cell. Thus, our findings reveal an additional layer of complexity in CarD's regulatory mechanism and could help explain how CarD expression *in vivo* could lead to differential gene expression outcomes in different conditions.

Discussion

CarD is an essential transcriptional regulator in *Mtb* that affects the expression of over two-thirds of the genome (8) and whose normal function and expression are required for bacterial survival during various stresses and virulence in mice (9, 10, 13, 48). Numerous *in vitro* studies have shown that CarD stabilizes RP_o formed by the housekeeping *Mtb*RNAP-σ^A holoenzyme (12, 15, 16), leading to the early model that it functions as a general transcription activator. However, a subsequent RNA-seq study of *Mtb* strains encoding mutant alleles of CarD revealed a more complex scenario where CarD appears to differentially activate or repress transcription from different promoters (8). In an effort to understand how CarD could affect gene expression in a promoter specific manner, we now provide experimental evidence for a relationship between RP_o stability and the outcome of CarD regulation that results in promoter specific effects of CarD activity. We find that the ratio of transcript production in multi-round transcription reactions ± CarD shows a roughly linear inverse correlation with increasing RP_o stability, with the most stable promoter variants ($AP3_{EcoExt}$, $AP3_{Stable}$, and $AP3_{Discr5}$) being transcriptionally repressed by CarD. CarD's effect on mycobacterial transcription *in vivo* also reflects the observations from our *in vitro* experiments where promoters predicted to be repressed by CarD are associated with sequence features that correlate with high RP_o stability (extended –10 sequence motif, low GC% discriminator region) and promoters predicted to be activated by CarD are associated with an absence of these features. Collectively, these data support our model in which the specific outcome of CarD-mediated RP_o stabilization is dependent on the kinetic properties of a given promoter and not on sequence-specific binding, which could explain the observed differential gene expression effects in CarD mutants *in vivo*.

Our study deepens our understanding of mycobacterial transcription regulation and demonstrates how RNAP-binding factors like CarD add complexity to this process. The true relationship between promoter sequence and CarD regulation is likely more nuanced than the data presented in this study. Although the AP3 promoter variants we generated were designed to increase or decrease RP_o stability in a stepwise manner (*i.e.*, $AP3_{Stable}$ is a combination of $AP3_{Discr}$ and $AP3_{ExoEct}$; G + C% is titrated one base at a time in $AP3_{Discr1}$-$AP3_{Discr5}$), the effects of each mutation are likely more complex. Minor base substitutions in a promoter sequence can result in large-scale allosteric effects on other RNAP–DNA interactions (49) and kinetic steps (50) outside of RP_o. Furthermore, our model was built on the idea that CarD uses a single kinetic mechanism, but CarD's effects on specific

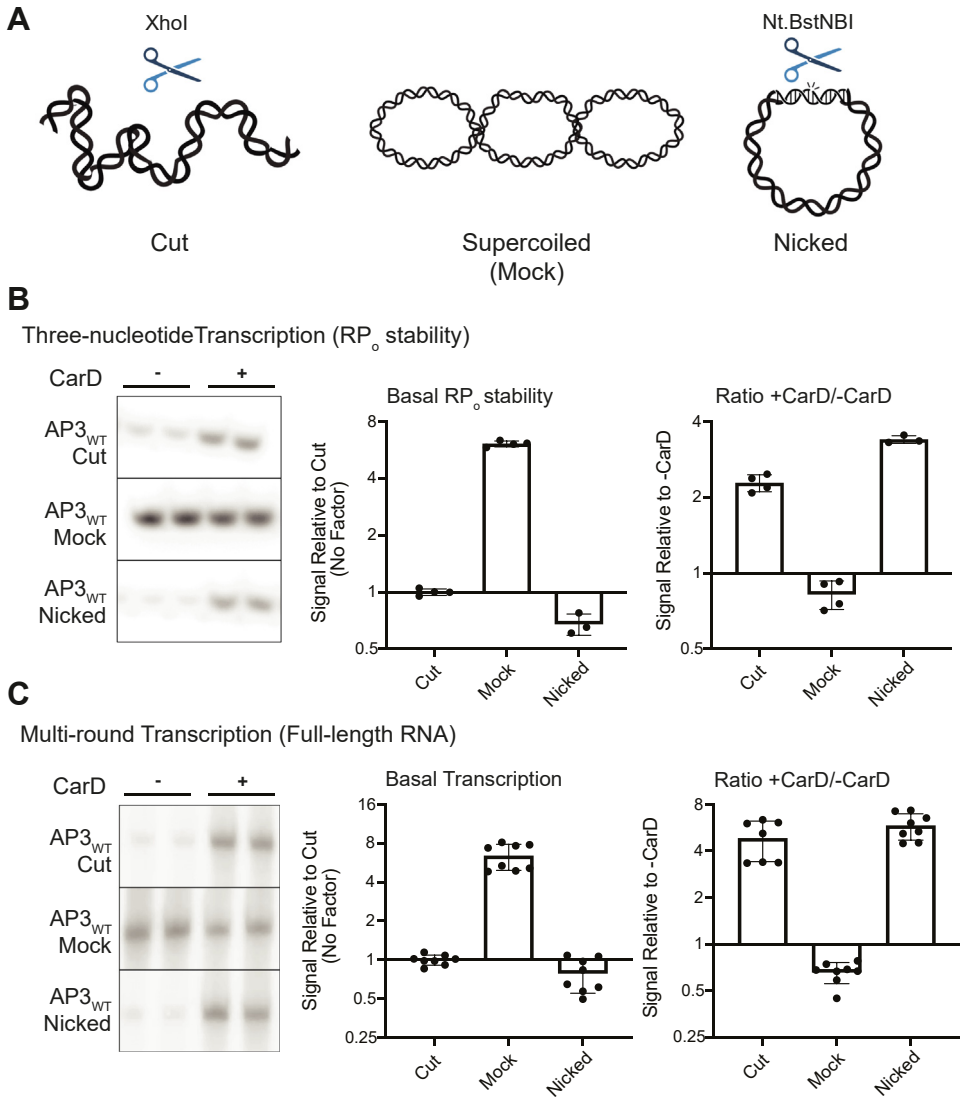

Figure 6. DNA topology affects the RP$_o$ stability of promoters and can alter the regulatory outcome of CarD. *A*, schematic of DNA templates used for *in vitro* transcription reactions. All templates transcribe an identical ~100-nucleotide RNA product from the wild-type *Mtb rrn*AP3 promoter (AP3$_{WT}$). Each DNA template originates from a negatively supercoiled plasmid that was treated with no enzyme (Mock), a nicking endonuclease (Nicked), or a single-cutting restriction endonuclease (Cut). *B*, representative gels showing [^{32}P]-labeled three-nucleotide transcription products formed by *Mtb*RNAP-σ^A from each DNA template either in the absence or presence of CarD. *C*, representative gels showing full-length [^{32}P]-labeled RNA transcripts produced by *Mtb*RNAP-σ^A from each DNA template in either the absence or presence of CarD. *B* and *C*, bar graphs display (*left*) the mean basal signal intensity relative to the linear "Cut" DNA template ± standard deviation (SD) and (*right*) the mean ratio of signal intensity +CarD/-CarD for each promoter ± SD. Group means were compared by one-way ANOVA $p < 0.0001$. The full results of pairwise comparisons are listed in Table S4. The raw gel images directly from the phosphorimager are shown in Figs. S5 and S6. AP3, *Mtb* ribosomal RNA promoter *rrn*AP3; *Mtb, Mycobacterium tuberculosis*; RNAP, RNA polymerase; RP$_o$, RNAP-promoter open complex.

transcription initiation rate constants may differ between promoters. For example, CarD contains a conserved tryptophan residue in its DBD (W85) that is positioned to interact with a T at the −12 position of the nontemplate DNA strand at the upstream fork of the bubble (12), and it has been hypothesized that this sequence-specific interaction acts as a "wedge" to prevent bubble collapse. In theory, on a promoter lacking T$_{-12}$, CarD's inhibitory effect on $k_{collapse}$ may be diminished relative to its effects on the rates of bubble opening and promoter escape, producing a unique kinetic mechanism that is biased toward repression. In our RNA-seq dataset, *Mtb* promoters that were predicted to be repressed by CarD were significantly enriched for non-T bases at the −12 position (8), lending some *in vivo* support for the prediction that this DNA sequence context biases CarD toward transcriptional repression.

The specific interaction between CarD W85 and T$_{-12}$ also raises the possibility that specific promoter DNA sequences could influence CarD's binding preference for partially opened promoter complexes. A recent study showed that CarD has poor binding affinity for RNAP or DNA alone (51), suggesting that CarD may bind to transcription initiation complexes after the initial association between RNAP and DNA. In our ChIP-seq dataset, *M. smegmatis* promoters associated with a primary TSS and containing a σ^A-like −10 element motif (A$_{-11}$NNNT$_{-7}$) that were within 100 bp of a CarD binding site were significantly

underenriched (hypergeometric test p = 5.66e-06) for promoters lacking a T_{-12} (22%; 93/429) compared to the genome-wide proportion (30%; 765/2511) (Tables S3 and S5). These data support the hypothesis that certain DNA sequence-specific interactions may influence but not determine the association between CarD and transcription complexes at specific mycobacterial promoters.

Another region that we did not study but could affect CarD regulation is the initially transcribed sequence downstream of the TSS, which can affect the kinetics of promoter escape and RNAP pausing (52–54). Simplistically, CarD represses transcription from certain promoters by overstabilizing RP_o and decreasing transcript flux by inhibiting promoter escape (7), leading to an accumulation of abortive transcripts (23). However, this model becomes more complicated when considering a branched pathway of transcription initiation (55), where a fraction of RNAP form moribund complexes that never undergo promoter escape. Kinetic studies using a fluorescent reporter showed that CarD increases the fraction of unescaped RNAP complexes (18), and we show that in some contexts, CarD can inhibit the synthesis of a three nucleotide product from RP_o. These data suggest that CarD could affect steps of initial nucleotide incorporation prior to promoter escape and influence the fraction of RNAP complexes undergoing productive *versus* moribund transcription (54, 56).

We also find that this relationship between RP_o stability and CarD is not only influenced by promoter sequence, where promoters with identical DNA sequence can be differentially activated or repressed depending on their supercoiling status (Fig. 6). In our experiments, CarD directly activated transcription from the *Mtb* rRNA promoter AP3 on a linear DNA template but repressed transcription from AP3 on a negatively supercoiled template (Fig. 6), which is the predominant topological state of DNA in bacterial cells (46). On the surface, this seems to contradict CarD's role as a positive regulator of rRNA synthesis *in vivo* (13, 20, 25, 57). However, one possible explanation may be that CarD is required to maintain efficient transcription of operons downstream of highly transcribed regions, such as the rRNA operon, when they accumulate positive supercoils due to their high transcriptional activity (46). We propose that CarD may function to overcome the topologically self-limiting nature of rRNA transcription to promote rapid bacterial growth.

Beyond its role in specifically regulating rRNA synthesis, CarD also affects the transcription of hundreds of other *Mtb* genes *in vivo* (8), which could explain CarD's pleiotropic effects under different stresses. *Mtb* strains with altered CarD activity are also sensitized to various environmental stresses other than nutrient starvation including oxidative stress, genotoxic stress, and antibiotic treatment (9, 10, 13, 48), but it is still unclear what roles CarD plays under these conditions. The impact of topology and promoter context also implies that CarD may elicit different effects on gene expression in different environments. CarD's ability to interpret the kinetic properties of a promoter add modularity to the mycobacterial transcription response, because while DNA sequence is essentially constant over the lifetime of a bacterial cell, its kinetic properties may be dynamic and responsive to environmental stimuli. *In vivo*, the supercoiling state of a promoter is constantly changing in response to the translocation of polymerases, the enzymatic action of topoisomerases, and DNA damage caused by antibiotics or other genotoxic stresses (46, 58). In addition to DNA supercoiling, other environmental factors such as intracellular NTP concentrations (59) and temperature (60) can influence the kinetic properties of a promoter without affecting DNA sequence. During pathogenesis, *Mtb* may encounter these environmental stimuli in various combinations. Furthermore, the expression of CarD is itself highly responsive to environmental signals, including nutrient limitation (48) and DNA damage (9). Understanding how transcription factors like CarD interact with these environmental stresses may provide insight into how *Mtb* responds to the host environment and antibiotic treatment, making this an intriguing direction of future study.

Based on the results of this study, we propose that CarD belongs to a growing class of RNAP-binding transcription factors that include DksA/(p)ppGpp (6, 61), TraR and its phage-encoded homologs (62, 63), and the σ-subunit interacting transcription factors including the Actinobacteria-specific protein RbpA (3, 64–67). Like CarD, these factors coordinate broad transcriptional programs in bacteria (5, 14, 65), highlighting the expanded regulatory range of these factors compared to classical transcription factors that are limited to promoters containing a specific binding motif. All of these global transcriptional regulators function by modulating the kinetics of transcription initiation, albeit *via* different mechanisms. Whereas CarD stabilizes RP_o, DksA/(p)ppGpp binds RNAP and destabilizes a kinetic intermediate preceding RP_o, resulting in transcriptional repression at ribosomal RNA promoters that form unstable RP_o and transcriptional activation at promoters of amino acid biosynthesis genes that form relatively stable RP_o (6, 61, 68–70). Although they exert opposite effects on initiation kinetics, CarD and DksA/(p)ppGpp share the ability to "read" the kinetic properties of a promoter to exert multiple regulatory outcomes on transcription. This study of CarD's regulatory mechanism demonstrates how kinetic context influences the activity of this class of RNAP-binding transcription factors and reveals another layer in how bacteria coordinate broad gene expression in response to their environment.

Experimental procedures

Bacterial growth and RNA collection

All *M. smegmatis* strains used in this study were derived from mc^2155 and grown in LB medium supplemented with 0.5% dextrose, 0.5% glycerol, and 0.05% Tween-80 at 37 °C. *M. smegmatis* strains expressing $CarD^{WT}$, $CarD^{R25E}$, $CarD^{K125E}$, or $CarD^{I27W}$ were engineered so that the native copy of *carD* is deleted, and the respective CarD allele is expressed from a constitutive P*myc1-tetO* promoter integrated into the genome. The construction of these strains has been previously described (13, 20). For RNA collection, *M. smegmatis* cultures were grown to A_{600} 0.5 to 0.9, pelleted,

and lysed in TRIzol reagent (Invitrogen) by bead-beating. RNA was isolated by TRIzol–chloroform extraction followed by isopropanol precipitation and finally resuspended in nuclease-free water (Invitrogen).

RNA sequencing and data analysis

RNA samples were DNase treated using the TURBO DNA-*free* Kit (Invitrogen) and submitted to the Washington University Genome Technology Access Center for paired-end Illumina sequencing (NovaSeq 6000 XP). Ribosomal RNA was depleted prior to sequencing using the Qiagen FastSelect system. Illumina reads were preprocessed using *FastQC*, and adapter sequences were removed using *trimmomatic* (71). Sequencing reads were aligned using *HiSat2* (72) to the *M. smegmatis* mc^2155 reference genome (assembly ASM1500v1) from the *Ensembl* database (73). Reads mapping to annotated protein coding regions were quantified using *featureCounts* (74). Differential expression analysis was performed using *DESeq2* (75). Downstream data analysis and visualization was performed using custom R scripts.

Protein purification

Plasmids containing the *M. tuberculosis* H37Rv genomic DNA encoding the different *Mtb* RNAP holoenzyme subunits were a gift from Jayanta Mukhopadhyay (Bose Institute). *Mtb*RNAP-σ^A holoenzyme was purified as previously described (65, 76). Briefly, *Mtb* *Mtb*RNAP-σ^A holoenzyme protein was expressed in *E. coli* BL21 cells containing the plasmids pET-Duet-*rpoB-rpoC* (encoding the β and β′ subunits), pAcYc-Duet-*sigA-rpoA* (encoding an N-terminal 10xHis-tagged-σ^A subunit and α subunits), and pCDF-*rpoZ* (encoding the ω subunit). Holoenzyme protein was isolated from *E. coli* cell lysate by affinity chromatography using a 2× 5 ml HisTrap HP Ni^{2+} affinity columns (Cytiva) and further purified by size-exclusion chromatography using a Sephacryl S-300 HiPrep column (Cytiva) to select for associated holoenzyme. Purified *Mtb*RNAP-σ^A holoenzyme was flash frozen in storage buffer (50% glycerol, 10 mM Tris pH 7.9, 200 mM NaCl, 0.1 mM EDTA, 1 mM $MgCl_2$, 20 μM ZnCl, and 2 mM DTT) and stored at −80 °C. CarD proteins were expressed in BL21 *E. coli* cells using the pET SUMO vector system described previously (65). Purified CarD protein was stored in 20 mM Tris pH 7.9, 150 mM NaCl, and 1 mM beta-mercaptoethanol.

In vitro *transcription*

Promoter fragments used for *in vitro* transcription were prepared by annealing two complementary single-stranded DNA oligos (IDT) containing the WT or variant AP3 promoter sequence from positions −39 to +4 relative to the transcription start site to create a linear double-stranded DNA fragment that was ligated into the pMSG434 plasmid. Linear DNA templates used for *in vitro* transcription were prepared PCR amplifying a 437 bp fragment from the pMSG434 plasmid. Plasmid DNA templates for *in vitro* transcription were constructed by inserting an intrinsic transcription termination sequence (5′-TTTAT-3′) into the pMSG434 plasmid 70 bp downstream of the cloned AP3 transcription start site. Negatively supercoiled plasmids were grown in *E. coli* and then isolated using a QIAGEN Plasmid Midi Kit. To generate cut or nicked plasmid templates, plasmid DNA was incubated with XhoI restriction endonuclease (NEB) at 37 °C or Bt.NstNBI nicking endonuclease (NEB) at 55 °C for 1 h, respectively. All DNA templates were purified by extracting with buffer-saturated phenol pH >7.4 (Invitrogen) followed by isopropanol precipitation before being used in *in vitro* transcription reactions. A full list of the primers used to construct the DNA templates can be found in Table S6.

Multiround *in vitro* transcription assays were performed by combining *Mtb*RNAP-σ^A holoenzyme, template DNA, and NTPs in a 20 μl reaction volume. Multiround reactions contained final concentrations of 40 nM RNAP holoenzyme, 0.8 nM DNA template, 0.1 mg/ml BSA, 1 mM DTT, 400 μM GTP, 200 μM ATP, 200 μM CTP, 200 μM UTP, 20 μCi/ml [α-^{32}P]-UTP (PerkinElmer), 10 mM Tris-HCl pH 7.9, 10 mM $MgCl_2$, and 40 mM NaCl. Reactions were initiated with the addition of NTPs and incubated at 37 °C for 1 h before being terminated with the addition of 20 μl 'stop buffer' (95% formamide and <0.1% bromophenol blue and xylene cyanol). Three nucleotide *in vitro* transcription reactions were performed in the same manner, except with final reaction concentrations of 100 nM RNAP holoenzyme, 10 nM DNA template, 0.1 mg/ml BSA, 1 mM DTT, 20 μM GpU, 10 μM UTP, 62.5 μCi/ml [α-^{32}P]-UTP, 10 mM Tris-HCl pH 7.9, 10 mM $MgCl_2$, and 40 mM NaCl. Multiround and three nucleotide *in vitro* transcription reaction products were separated by gel electrophoresis on denaturing (7M urea) 8% or 22% polyacrylamide gels, respectively, which were vacuum dried and visualized using a phosphorimager screen. Reactions with CarD contained 25:1 M ratio CarD:RNAP (1 μM CarD for the multiround *in vitro* transcription reactions or 2.5 μM CarD for the three nucleotide transcription reactions) unless otherwise noted. All original unprocessed gel images can be found in Figs. S5 and S6.

Data availability

Raw RNA-seq data have been deposited in the GEO repository under accession code GSE222815.

Supporting information—This article contains supporting information (21, 24, 44, 75).

Acknowledgments—We thank Drake Jensen, Ana Ruiz Manzano, and Eric Galburt for their helpful discussions and for providing the *E. coli* protein expression strain for *Mtb*RNAP-σ^A purification. We also thank John Errico, Helen Blaine, and Daved Fremont for their help in purification of RNA polymerase.

Author contributions—D. X. Z. and C. L. S. conceptualization; D. X. Z. and C. L. S. methodology; D. X. Z. validation; D. X. Z. formal analysis; D. X. Z. investigation; D. X. Z. and C. L. S. writing—original draft; D. X. Z. and C. L. S. writing—review & editing; D. X.

Z. and C. L. S. visualization; C. L. S. resources; C. L. S. supervision; C. L. S. project administration; C. L. S. funding acquisition.

Funding and additional information—This work was supported by NIH NIGMS grant GM107544 and a Burroughs Wellcome Fund Investigator in the Pathogenesis of Infectious Disease Award awarded to C. L. S. D. X. Z. is supported by NIH NIAID grant T32A1007172. We also thank the Genome Technology Access Center at the McDonnell Genome Institute at Washington University School of Medicine. The Center is partially supported by NCI Cancer Center Support Grant #P30 CA91842 to the Siteman Cancer Center and by ICTS/CTSA Grant# UL1TR002345 from the National Center for Research Resources (NCRR), a component of the National Institutes of Health (NIH), and NIH Roadmap for Medical Research. This publication is solely the responsibility of the authors and does not necessarily represent the official view of NCRR or NIH.

Conflict of interest—The authors declare that they have no conflict of interest with the contents of this article.

Abbreviations—The abbreviations used are: AP3, *Mtb* ribosomal RNA promoter *rrn*AP3; ChIP-seq, chromatin immunoprecipitation sequencing; DBD, DNA-binding domain; *Mtb*, *Mycobacterium tuberculosis*; RNAP, RNA polymerase; RID, RNAP-interaction domain; RP_o, RNAP-promoter open complex; RP_c, RNAP-promoter closed complexes; RNA-seq, RNA-sequencing; TSS, transcription start site.

References

1. Flentie, K., Garner, A. L., and Stallings, C. L. (2016) Mycobacterium tuberculosis transcription machinery: ready to respond to host attacks. *J. Bacteriol.* **198**, 1360–1373
2. Minch, K. J., Rustad, T. R., Peterson, E. J. R., Winkler, J., Reiss, D. J., Ma, S., *et al.* (2015) The DNA-binding network of Mycobacterium tuberculosis. *Nat. Commun.* **6**, 5829
3. Vishwakarma, R. K., and Brodolin, K. (2020) The σ subunit-remodeling factors: an emerging paradigms of transcription regulation. *Front. Microbiol.* **11**, 1798
4. Haugen, S. P., Ross, W., and Gourse, R. L. (2008) Advances in bacterial promoter recognition and its control by factors that do not bind DNA. *Nat. Rev. Microbiol.* **6**, 507–519
5. Sanchez-Vazquez, P., Dewey, C. N., Kitten, N., Ross, W., and Gourse, R. L. (2019) Genome-wide effects on Escherichia coli transcription from ppGpp binding to its two sites on RNA polymerase. *Proc. Natl. Acad. Sci. U. S. A.* **116**, 8310–8319
6. Paul, B. J., Berkmen, M. B., and Gourse, R. L. (2005) DksA potentiates direct activation of amino acid promoters by ppGpp. *Proc. Natl. Acad. Sci. U. S. A.* **102**, 7823–7828
7. Galburt, E. A. (2018) The calculation of transcript flux ratios reveals single regulatory mechanisms capable of activation and repression. *Proc. Natl. Acad. Sci. U. S. A.* **115**, E11604–E11613
8. Zhu, D. X., Garner, A. L., Galburt, E. A., and Stallings, C. L. (2019) CarD contributes to diverse gene expression outcomes throughout the genome of Mycobacterium tuberculosis. *Proc. Natl. Acad. Sci. U. S. A.* **116**, 13573–13581
9. Stallings, C. L., Stephanou, N. C., Chu, L., Hochschild, A., Nickels, B. E., and Glickman, M. S. (2009) CarD is an essential regulator of rRNA transcription required for Mycobacterium tuberculosis persistence. *Cell* **138**, 146–159
10. Weiss, L. A., Harrison, P. G., Nickels, B. E., Glickman, M. S., Campbell, E. A., Darst, S. A., *et al.* (2012) Interaction of CarD with RNA polymerase mediates Mycobacterium tuberculosis viability, rifampin resistance, and pathogenesis. *J. Bacteriol.* **194**, 5621–5631
11. Boyaci, H., Chen, J., Jansen, R., Darst, S. A., and Campbell, E. A. (2019) Structures of an RNA polymerase promoter melting intermediate elucidate DNA unwinding. *Nature* **565**, 382–385
12. Bae, B., Chen, J., Davis, E., Leon, K., Darst, S. A., and Campbell, E. A. (2015) CarD uses a minor groove wedge mechanism to stabilize the RNA polymerase open promoter complex. *Elife* **4**, e08505
13. Garner, A. L., Weiss, L. A., Manzano, A. R., Galburt, E. A., and Stallings, C. L. (2014) CarD integrates three functional modules to promote efficient transcription, antibiotic tolerance, and pathogenesis in mycobacteria. *Mol. Microbiol.* **93**, 682–697
14. Hubin, E. A., Fay, A., Xu, C., Bean, J. M., Saecker, R. M., Glickman, M. S., *et al.* (2017) Structure and function of the mycobacterial transcription initiation complex with the essential regulator RbpA. *Elife* **6**, e22520
15. Rammohan, J., Manzano, A. R., Garner, A. L., Stallings, C. L., and Galburt, E. A. (2015) CarD stabilizes mycobacterial open complexes *via* a two-tiered kinetic mechanism. *Nucl. Acids Res.* **43**, 3272–3285
16. Davis, E., Chen, J., Leon, K., Darst, S. A., and Campbell, E. A. (2015) Mycobacterial RNA polymerase forms unstable open promoter complexes that are stabilized by CarD. *Nucl. Acids Res.* **43**, 433–445
17. Srivastava, D. B., Leon, K., Osmundson, J., Garner, A. L., Weiss, L. A., Westblade, L. F., *et al.* (2013) Structure and function of CarD, an essential mycobacterial transcription factor. *Proc. Natl. Acad. Sci. U. S. A.* **110**, 12619–12624
18. Jensen, D., Manzano, A. R., Rammohan, J., Stallings, C. L., and Galburt, E. A. (2019) CarD and RbpA modify the kinetics of initial transcription and slow promoter escape of the Mycobacterium tuberculosis RNA polymerase. *Nucl. Acids Res.* **47**, 6685–6698
19. Rammohan, J., Ruiz Manzano, A., Garner, A. L., Prusa, J., Stallings, C. L., and Galburt, E. A. (2016) Cooperative stabilization of Mycobacterium tuberculosis rrnA P3 promoter open complexes by RbpA and CarD. *Nucl. Acids Res.* **44**, gkw577
20. Garner, A. L., Rammohan, J., Huynh, J. P., Onder, L. M., Chen, J., Bae, B., *et al.* (2017) Effects of increasing the affinity of CarD for RNA polymerase on Mycobacterium tuberculosis growth, rRNA transcription, and virulence. *J. Bacteriol.* https://doi.org/10.1128/JB.00698-16
21. Landick, R., Krek, A., Glickman, M. S., Socci, N. D., and Stallings, C. L. (2014) Genome-wide mapping of the distribution of CarD, RNAP σ(A), and RNAP β on the Mycobacterium smegmatis chromosome using chromatin immunoprecipitation sequencing. *Genomics Data* **2**, 110–113
22. Henry, K. K., Ross, W., Myers, K. S., Lemmer, K. C., Vera, J. M., Landick, R., *et al.* (2020) A majority of Rhodobacter sphaeroides promoters lack a crucial RNA polymerase recognition feature, enabling coordinated transcription activation. *Proc. Natl. Acad. Sci. U. S. A.* **117**, 29658–29668
23. Henry, K. K., Ross, W., and Gourse, R. L. (2021) Rhodobacter sphaeroides card negatively regulates its own promoter. *J. Bacteriol.* https://doi.org/10.1128/JB.00210-21
24. Martini, M. C., Zhou, Y., Sun, H., and Shell, S. S. (2019) Defining the transcriptional and post-transcriptional landscapes of mycobacterium smegmatisin aerobic growth and hypoxia. *Front. Microbiol.* **10**, 1–17
25. Woldemeskel, S. A., Daitch, A. K., Alvarez, L., Panis, G., Zeinert, R., Gonzalez, D., *et al.* (2020) The conserved transcriptional regulator CdnL is required for metabolic homeostasis and morphogenesis in Caulobacter. *PLoS Genet.* **16**, e1008591
26. Jensen, D., and Galburt, E. A. (2021) The context-dependent influence of promoter sequence motifs on transcription initiation kinetics and regulation. *J. Bacteriol.* **203**, e00512-20
27. Lee, J., and Borukhov, S. (2016) Bacterial RNA polymerase-DNA interaction-The driving force of gene expression and the target for drug action. *Front. Mol. Biosci.* https://doi.org/10.3389/fmolb.2016.00073
28. Bae, B., Feklistov, A., Lass-Napiorkowska, A., Landick, R., and Darst, S. A. (2015) Structure of a bacterial RNA polymerase holoenzyme open promoter complex. *Elife* **4**, e08504
29. Newton-Foot, M., and Gey van Pittius, N. C. (2013) The complex architecture of mycobacterial promoters. *Tuberculosis (Edinb).* **93**, 60–74
30. Campbell, E. A., Muzzin, O., Chlenov, M., Sun, J. L., Olson, C. A., Weinman, O., *et al.* (2002) Structure of the bacterial RNA polymerase promoter specificity σ subunit. *Mol. Cell.* **9**, 527–539

31. Chen, J., Chiu, C., Gopalkrishnan, S., Chen, A. Y., Olinares, P. D. B., Saecker, R. M., *et al.* (2020) Stepwise promoter melting by bacterial RNA polymerase. *Mol. Cell.* **78**, 275–288.e6
32. Feklistov, A., and Darst, S. A. (2011) Structural basis for promoter-10 element recognition by the bacterial RNA polymerase σ subunit. *Cell* **147**, 1257–1269
33. Keilty, S., and Rosenberg, M. (1987) Constitutive function of a positively regulated promoter reveals new sequences essential for activity. *J. Biol. Chem.* **262**, 6389–6395
34. Zhu, Y., Mao, C., Ge, X., Wang, Z., and Lu, P. (2017) Characterization of a minimal type of position in Mycobacteria. *J. Bacteriol.* **199**. https://doi.org/10.1128/JB.00385-17
35. Hubin, E. A., Lilic, M., Darst, S. A., and Campbell, E. A. (2017) Structural insights into the mycobacteria transcription initiation complex from analysis of X-ray crystal structures. *Nat. Commun.* **8**, 16072
36. Feklistov, A., Barinova, N., Sevostyanova, A., Heyduk, E., Bass, I., Vvedenskaya, I., *et al.* (2006) A basal promoter element recognized by free RNA polymerase σ subunit determines promoter recognition by RNA polymerase holoenzyme. *Mol. Cell.* **23**, 97–107
37. Haugen, S. P., Berkmen, M. B., Ross, W., Gaal, T., Ward, C., and Gourse, R. L. (2006) rRNA promoter regulation by nonoptimal binding of σ region 1.2: an additional recognition element for RNA polymerase. *Cell* **125**, 1069–1082
38. Barinova, N., Kuznedelov, K., Severinov, K., and Kulbachinskiy, A. (2008) Structural modules of RNA polymerase required for transcription from promoters containing downstream basal promoter element GGGA. *J. Biol. Chem.* **283**, 22482–22489
39. Zuo, Y., and Steitz, T. A. (2015) Crystal structures of the e.coli transcription initiation complexes with a complete bubble. *Mol. Cell.* **58**, 534–540
40. Yakovchuk, P., Protozanova, E., and Frank-Kamenetskii, M. D. (2006) Base-stacking and base-pairing contributions into thermal stability of the DNA double helix. *Nucl. Acids Res.* **34**, 564–574
41. Wang, A. H. J., Hakoshima, T., van der Marel, G., van Boom, J. H., and Rich, A. (1984) AT base pairs are less stable than GC base pairs in Z-DNA: the crystal structure of d(m5CGTAm5CG). *Cell* **37**, 321–331
42. Pemberton, I. K., Muskhelishvili, G., Travers, A. A., Buckle, M., and Physicochimie, Â. De (2000) The G+C-rich discriminator region of the tyrT promoter antagonises the formation of stable preinitiation complexes. *J. Mol. Biol.* https://doi.org/10.1006/jmbi.2000.3780
43. Gummesson, B., Lovmar, M., and Nyström, T. (2013) A proximal promoter element required for positive transcriptional control by guanosine tetraphosphate and DKSA protein during the stringent response. *J. Biol. Chem.* **288**, 21055–21064
44. Cortes, T., Schubert, O. T., Rose, G., Arnvig, K. B., Comas, I., Aebersold, R., *et al.* (2013) Genome-wide mapping of transcriptional start sites defines an extensive leaderless transcriptome in Mycobacterium tuberculosis. *Cell Rep.* **5**, 1121–1131
45. Shell, S. S., Wang, J., Lapierre, P., Mir, M., Chase, M. R., Pyle, M. M., *et al.* (2015) Leaderless transcripts and small proteins are common features of the mycobacterial translational landscape. *PLoS Genet.* **11**, e1005641
46. Dorman, C. J. (2019) DNA supercoiling and transcription in bacteria: a two-way street. *BMC Mol. Cell Biol.* **20**, 26
47. Revyakin, A., Ebright, R. H., and Strick, T. R. (2004) Promoter unwinding and promoter clearance by RNA polymerase: detection by single-molecule DNA nanomanipulation. *Proc. Natl. Acad. Sci. U. S. A.* **101**, 4776–4780
48. Li, X., Chen, F., Liu, X., Xiao, J., Andongma, B. T., Tang, Q., *et al.* (2022) Clp protease and antisense RNA jointly regulate the global regulator CarD to mediate mycobacterial starvation response. *Elife* **11**, e73347
49. Saecker, R. M., Chen, J., Chiu, C. E., Malone, B., Sotiris, J., Ebrahim, M., *et al.* (2021) Structural origins of Escherichia coli RNA polymerase open promoter complex stability. *Proc. Natl. Acad. Sci. U. S. A.* **118**, e2112877118
50. Petushkov, I., Pupov, D., Bass, I., and Kulbachinskiy, A. (2015) Mutations in the CRE pocket of bacterial RNA polymerase affect multiple steps of transcription. *Nucl. Acids Res.* **43**, 5798–5809
51. Stefan, M. A., Velazquez, G. M., and Garcia, G. A. (2020) High-throughput screening to discover inhibitors of the CarD·RNA polymerase protein–protein interaction in Mycobacterium tuberculosis. *Sci. Rep.* **10**, 21309
52. Heyduk, E., and Heyduk, T. (2018) DNA template sequence control of bacterial RNA polymerase escape from the promoter. *Nucl. Acids Res.* **46**, 4469–4486
53. Ko, J., and Heyduk, T. (2014) Kinetics of promoter escape by bacterial RNA polymerase: effects of promoter contacts and transcription bubble collapse. *Biochem. J.* **463**, 135–144
54. Henderson, K. L., Felth, L. C., Molzahn, C. M., Shkel, I., Wang, S., Chhabra, M., *et al.* (2017) Mechanism of transcription initiation and promoter escape by *E . coli* RNA polymerase. *Proc. Natl. Acad. Sci. U. S. A.* **114**, E3032–E3040
55. Susa, M., Sen, R., and Shimamoto, N. (2002) Generality of the branched pathway in transcription initiation by Escherichia coli RNA polymerase. *J. Biol. Chem.* **277**, 15407–15412
56. Dulin, D., Bauer, D. L. V., Malinen, A. M., Bakermans, J. J. W., Kaller, M., Morichaud, Z., *et al.* (2018) Pausing controls branching between productive and non-productive pathways during initial transcription in bacteria. *Nat. Commun.* **9**, 1478
57. Chen, T., Xiang, X., Xu, H., Zhang, X., Zhou, B., Yang, Y., *et al.* (2018) LtpA, a CdnL-type CarD regulator, is important for the enzootic cycle of the Lyme disease pathogen. *Emerg. Microbes Infect.* **7**, 126
58. Dorman, C. J., and Dorman, M. J. (2016) DNA supercoiling is a fundamental regulatory principle in the control of bacterial gene expression. *Biophys. Rev.* **8**, 89–100
59. Gaal, T., Bartlett, M. S., Ross, W., Turnbough, C. L., and Gourse, R. L. (1997) Transcription regulation by initiating NTP concentration: rRNA synthesis in bacteria. *Science* **278**, 2092–2097
60. Plaskon, D. M., Henderson, K. L., Felth, L. C., Molzahn, C. M., Evensen, C., Dyke, S., *et al.* (2021) Temperature effects on RNA polymerase initiation kinetics reveal which open complex initiates and that bubble collapse is stepwise. *Proc. Natl. Acad. Sci. U. S. A.* **118**, e2021941118
61. Paul, B. J., Barker, M. M., Ross, W., Schneider, D. A., Webb, C., Foster, J. W., *et al.* (2004) DksA: a critical component of the transcription initiation machinery that potentiates the regulation of rRNA promoters by ppGpp and the initiating NTP. *Cell* **118**, 311–322
62. Chen, J., Gopalkrishnan, S., Chiu, C., Chen, A. Y., Campbell, E. A., Gourse, R. L., *et al.* (2019) E. Coli trar allosterically regulates transcription initiation by altering RNA polymerase conformation. *Elife* **8**, e49375
63. Gopalkrishnan, S., Ross, W., Akbari, M. S., Li, X., Haycocks, J. R. J., Grainger, D. C., *et al.* (2022) Homologs of the Escherichia coli F element protein TraR, including phage lambda Orf73, directly reprogram host transcription. *MBio* **13**, e0095222
64. Hu, Y., Morichaud, Z., Chen, S., Leonetti, J.-P., and Brodolin, K. (2012) Mycobacterium tuberculosis RbpA protein is a new type of transcriptional activator that stabilizes the σ A-containing RNA polymerase holoenzyme. *Nucl. Acids Res.* **40**, 6547–6557
65. Prusa, J., Jensen, D., Santiago-Collazo, G., Pope, S. S., Garner, A. L., Miller, J. J., *et al.* (2018) Domains within RbpA serve specific functional roles that regulate the expression of distinct mycobacterial gene subsets. *J. Bacteriol.* **200**, e00690-17
66. Bortoluzzi, A., Muskett, F. W., Waters, L. C., Addis, P. W., Rieck, B., Munder, T., *et al.* (2013) Mycobacterium tuberculosis RNA polymerase-binding protein A (RbpA) and its interactions with sigma factors. *J. Biol. Chem.* **288**, 14438–14450
67. Hubin, E. A., Tabib-Salazar, A., Humphrey, L. J., Flack, J. E., Olinares, P. D. B., Darst, S. A., *et al.* (2015) Structural, functional, and genetic analyses of the actinobacterial transcription factor RbpA. *Proc. Natl. Acad. Sci. U. S. A.* **112**, 7171–7176
68. Lemke, J. J., Sanchez-Vazquez, P., Burgos, H. L., Hedberg, G., Ross, W., and Gourse, R. L. (2011) Direct regulation of Escherichia coli ribosomal protein promoters by the transcription factors ppGpp and DksA. *Proc. Natl. Acad. Sci. U. S. A.* **108**, 5712
69. Rutherford, S. T., Villers, C. L., Lee, J., Ross, W., and Gourse, R. L. (2009) Allosteric control of Escherichia coli rRNA promoter complexes by DksA. *Genes Dev.* **23**, 236–248. https://doi.org/10.1101/gad.1745409

70. Gourse, R. L., Chen, A. Y., Gopalkrishnan, S., Sanchez-Vazquez, P., Myers, A., and Ross, W. (2018) Transcriptional responses to ppGpp and DksA. *Annu. Rev. Microbiol.* **72**, 163–184
71. Bolger, A. M., Lohse, M., and Usadel, B. (2014) Trimmomatic: a flexible trimmer for Illumina sequence data. *Bioinformatics* **30**, 2114–2120
72. Kim, D., Paggi, J. M., Park, C., Bennett, C., and Salzberg, S. L. (2019) Graph-based genome alignment and genotyping with HISAT2 and HISAT-genotype. *Nat. Biotechnol.* **37**, 907–915
73. Cunningham, F., Allen, J. E., Allen, J., Alvarez-Jarreta, J., Amode, M. R., Armean, I. M., *et al.* (2022) Ensembl 2022. *Nucl. Acids Res.* **50**, D988–D995
74. Liao, Y., Smyth, G. K., and Shi, W. (2014) FeatureCounts: an efficient general purpose program for assigning sequence reads to genomic features. *Bioinformatics* **30**, 923–930
75. Love, M. I., Huber, W., and Anders, S. (2014) Moderated estimation of fold change and dispersion for RNA-seq data with DESeq2. *Genome Biol.* **15**, 550
76. Banerjee, R., Rudra, P., Prajapati, R. K., Sengupta, S., and Mukhopadhyay, J. (2014) Optimization of recombinant Mycobacterium tuberculosis RNA polymerase expression and purification. *Tuberculosis* **94**, 397–404